SCIENTIFIC REPORTS

OPEN

SUBJECT AREAS:
SOLITONS
NONLINEAR OPTICS
ULTRAFAST PHOTONICS
SUPERCONTINUUM GENERATION

Received
22 October 2012

Accepted
15 November 2012

Published
6 December 2012

Correspondence and requests for materials should be addressed to D.F. (d.faccio@hw.ac.uk)

Soliton-induced relativistic-scattering and amplification

E. Rubino[1], A. Lotti[1,2], F. Belgiorno[3], S. L. Cacciatori[1], A. Couairon[2], U. Leonhardt[4] & D. Faccio[5]

[1]Dipartimento di Scienza e Alta Tecnologia, Università dell'Insubria, Via Valleggio 11, IT-22100 Como, Italy, [2]Centre de Physique Theorique CNRS, Ecole Polytechnique, F-91128 Palaiseau, France, [3]Dipartimento di Matematica, Politecnico di Milano, Piazza Leonardo 32, 20133 Milano, Italy, [4]School of Physics and Astronomy, University of St Andrews, North Haugh, St Andrews KY16 9SS, UK, [5]School of Engineering and Physical Sciences, SUPA, Heriot-Watt University, Edinburgh EH14 4AS, UK.

Solitons are of fundamental importance in photonics due to applications in optical data transmission and also as a tool for investigating novel phenomena ranging from light generation at new frequencies and wave-trapping to rogue waves. Solitons are also moving scatterers: they generate refractive index perturbations moving at the speed of light. Here we found that such perturbations scatter light in an unusual way: they amplify light by the mixing of positive and negative frequencies, as we describe using a first Born approximation and numerical simulations. The simplest scenario in which these effects may be observed is within the initial stages of optical soliton propagation: a steep shock front develops that may efficiently scatter a second, weaker probe pulse into relatively intense positive and negative frequency modes with amplification at the expense of the soliton. Our results show a novel all-optical amplification scheme that relies on soliton induced scattering.

If compared to the well-developed field of traditional light scattering in which the medium is at rest, little attention has been devoted to the physics of scattering from a moving medium, in particular from a relativistically moving medium. Here we consider the remarkable ability of solitons to generate a co-propagating refractive index inhomogeneity that propagates at relativistic speeds. The basics of scattering from a time-changing boundary were discussed in detail by Mendonça and co-workers (see e.g.[1] and references therein). Examples of such "time refraction" have been predicted and observed from a moving plasma front[1–3] and in waveguide structures[4–6]. Recently, the nonlinear Kerr effect, i.e. the local increase of the medium refractive index induced by an intense laser pulse[7], was proposed to induce a moving refractive index inhomogeneity within a dispersive medium such as an optical fibre[8]. The laser pulse induced relativistic inhomogeneity (RI) was then described in terms of a flowing medium in which the analogue of an event horizon may form[8] and applications such a optical transistors have been proposed[9].

Intense laser pulses are also known to scatter from the self-induced travelling RI: this self-scattering process leads to the resonant transfer of energy from the laser pulse to a significantly blue-shifted peak, often referred to as resonant radiation (RR) or "optical Cherenkov" radiation[10–14]. A recent discovery highlighted an additional scattered mode, further blue-shifted with respect to the RR, identified as a mode excited on the negative frequency branch of the medium dispersion relation and therefore named "negative resonant radiation" (NRR)[15].

By applying a first Born approximation analysis, supported by numerical simulations, we show that the scattering of light by a soliton induced RI reveals a novel all-optical amplification mechanism. A schematic representation of the specific process we are considering is shown in Fig. 1: an incoming laser pulse, IN, interacts with a co-propagating inhomogeneity, or scatterer. The momentum conservation law that governs the scattering process predicts that light may resonantly scatter into two output modes, RR and NRR (see SI for details). In the laboratory reference frame, both of these modes will have positive frequencies while in the reference frame comoving with the scatterer, RR is positive and NRR is negative valued. The key point in the following is precisely the presence of these two modes: mixing between the RR and NRR modes leads to a novel amplification process.

Results

First born approximation. In scattering theory, the first Born approximation allows us to estimate the elements of the scattering matrix **S**, which connects asymptotic input and output states. Kolesik *et al.* have shown that the positive RR mode is captured in great detail by the Born scattering approach[16]. Here we extend this theory in order to also include the possibility of scattering to the NRR mode and find that the amplitude of each scattering channel is proportional to the amplitude of the Fourier component of the RI, $\hat{R}(\omega)$ (see SI):

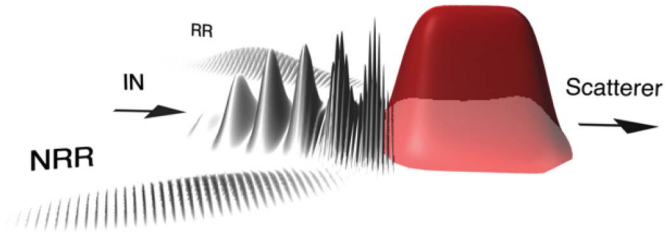

Figure 1 | Schematic representation of scattering from a relativistic inhomogeneity. An incoming laser pulse, IN, interacts with a co-propagating RI, or scatterer, that transfers energy into two output modes, RR and NRR.

$$S(z,\omega_{RR}) \approx \frac{v}{2}\hat{R}(\omega_{RR}-\omega_{IN}) \quad (1)$$

and, accounting also for the negative frequency branch, we similarly obtain:

$$S(z,\omega_{NRR}) \approx \frac{v}{2}\hat{R}(\omega_{NRR}+\omega_{IN}), \quad (2)$$

where v is the velocity of the travelling RI. These relations (1) and (2) state that energy may be transferred to *two* modes, RR and NRR, and in order to do so the spectrum of the scattering potential must have non-zero Fourier components at frequencies equal to the relative distances between ω_{IN} and the resonant frequencies. In other words, the RI must present a sufficiently steep gradient so as to effectively excite the desired output modes. We now observe that we may derive a photon number balance equation by generalizing the Manley-Rowe relation, adopted e.g. in nonlinear optics[7], to the case of a *moving* scatterer[17,18]. We find that:

$$|RR|^2 - |NRR|^2 = 1, \quad (3)$$

where $|RR|^2$ and $|NRR|^2$ are the photon numbers of the RR and NRR modes normalized to the input photon number, $|IN|^2$. The negative sign in front of the $|NRR|^2$ photon number is a direct consequence of the fact that the NRR-mode has negative frequency in the comoving reference frame (see SI). So the *difference* between the normalized number of photons has to be equal to the photon number in the input mode. As a consequence, the total output photon number, $|RR|^2 + |NRR|^2 > 1$, i.e. we have amplification. The scattering process mediated by the travelling RI will amplify photons as a result of the coupling between the positive and negative frequency modes.

Numerical simulations. We verified our predictions by numerically simulating the one dimensional propagation of a scalar field propagating along the z direction[19] in a transparent and isotropic dielectric medium (diamond and fused silica) that is arranged to scatter from a co-propagating inhomogeneity (see Methods). We consider three separate cases: (i) the underlying physics are first exemplified by taking a "toy-model" situation in which the RI is simply a variation in the linear refractive index; (ii) the RI is generated by an actual soliton-like laser pulse through the nonlinear Kerr effect and light from the soliton itself is self-scattered; (iii) the RI is generated by a soliton-like pulse and a second, very weak probe pulse is scattered by the soliton.

(i) - *"Toy-model" RI.* The RI is simulated as a linear propagating refractive index inhomogeneity that moves with a speed $v = 1.23 \times 10^8$ m/s that is just slightly slower than the group velocity of an input probe pulse in the medium, $v_g = 1.25 \times 10^8$ m/s. In this case, as a dielectric medium we choose diamond, which does not exhibit any resonances over a very broad bandwidth (from less than one Terahertz through to ultraviolet wavelengths). The probe pulse is very weak so that no nonlinear effects are excited and the physics are dominated solely by linear scattering from the RI. Figures 2(a)–(b) show the evolution along propagation of the envelope (plotted in the frame moving at the RI velocity) and of the spectrum, respectively. We launch an input Gaussian probe pulse (carrier wavelength 2 μm, pulse width 20 fs), together with a super-Gaussian shaped RI (see Methods), with amplitude $\delta n_0 = 0.08$ and super-Gaussian order $m = 40$ corresponding to a rising time ~ 3 fs; $\sigma = 50$ fs. This ensures a wide RI Fourier spectrum $\widehat{\delta n}(\omega)$, so as to meet both conditions (1) and (2). After ~ 0.2 mm the probe pulse reaches the moving RI [whose position is highlighted in Fig. 2(a) by the vertical black dotted lines] and slows down due to the RI increase of refractive index. Scattering occurs towards *two* blue-shifted resonant modes, RR and NRR, which due to dispersion both travel slower than the RI. The medium dispersion relation is shown in Fig. 2(d) in (ω', ω) coordinates where the comoving frequency $\omega' = \gamma(\omega - vk)$; $k =$

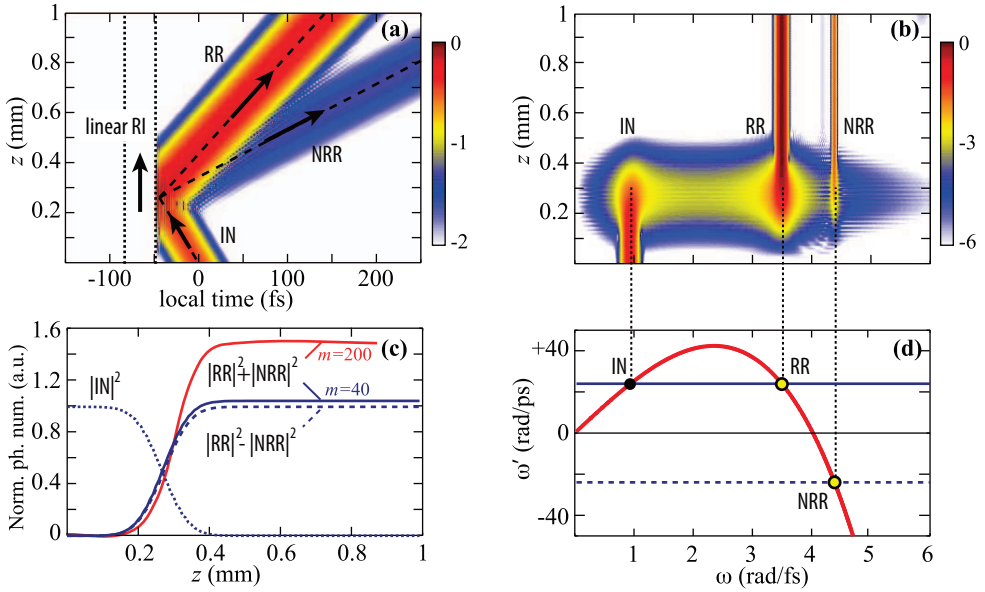

Figure 2 | Scattering from a "toy-model" RI in diamond: IN pulse at 2 μm; super-Gaussian moving RI with $m = 40$ (3 fs rise-time), $\delta n_0 = 0.08$. Envelope (a) and spectral (b) evolution along propagation. (c) Photon number evolution along propagation: the total sum (photon number amplification) increases with increasing RI steepness (increasing parameter m). (d) Comoving dispersion curve with indicated the allowed optical modes.

$\omega n(\omega)/c$ is the medium dispersion relation and $\gamma = 1/\sqrt{1-(v/c)^2}$, being c the speed of light in vacuum. In the comoving frame, the absolute value of scattered mode frequencies are determined by the input mode comoving frequency (horizontal solid and dashed lines, see SI): the corresponding laboratory reference frame frequencies can be seen to be in perfect agreement with the numerically observed values.

In order to verify the photon number amplification predicted by the Manley-Rowe relation (3), we evaluated the photon number evolution, as shown in Fig. 2(c) for two different RI gradients, obtained by varying the order of the super-Gaussian function that describes the RI, $m = 40$ and $m = 200$ (these correspond to rise times from the background refractive index to the maximum of the RI of 3 fs and 0.7 fs, respectively). Dotted, solid and dashed lines correspond to the normalized photon numbers in the IN mode, total output photons $|RR|^2 + |NRR|^2$ and output photon difference $|RR|^2 - |NRR|^2$, respectively. As can be seen, the difference in photon numbers is conserved while the sum of photon numbers is larger than 1 (amplification) and increases with increasing RI steepness. This simplified "toy-model" therefore gives a direct confirmation of the predictions based on the first Born approximation model.

(ii) - *Soliton-induced RI*. The RI is physically generated by an intense soliton-like laser pulse through the nonlinear Kerr effect, i.e. $\delta n = n_2 I$, where I is the peak intensity and n_2 the nonlinear Kerr coefficient (see Methods). The soliton may interact with the self-induced refractive index variation and scatter into new output modes. As a Kerr medium we choose common fused silica glass, whose dispersion relation is well known[20]. We launch a soliton-like mode in the anomalous dispersion region, with central wavelength 2 μm, pulse width 7 fs and input intensity 10 TW/cm^2. Figures 3(a)–(b) show the envelope and spectral evolution, respectively, along propagation over a distance $z = 0.4$ cm. The input pulse initially self-steepens, forms a shock front and, at $z \sim 0.3$ mm, when conditions (1)–(2) are met, energy starts to resonantly transfer from the input mode towards two blue-shifted modes, RR and NRR, both travelling slower with respect to the input soliton. The soliton frequency is red-shifted due to a recoil effect[10] and subsequently emerges with a slightly lower propagation velocity. In Figure 3(c)–(d) we compare the nonlinear propagation with a numerical simulation in which the nonlinear source term has been replaced with a RI in the *linear* polarization with the same amplitude, steepness and propagation velocity of the soliton induced perturbation of Figs. 3(a)–(b). We observe a nearly perfect agreement with the nonlinear case confirming that soliton shedding of RR and NRR modes is nothing more than a specific realization of the more general relativistic scattering process. The "toy-model" RI scattering is indeed able to capture all the essential features of the resonant energy transfer, and coupling between positive and negative frequency modes.

(iii) - *Probe pulse scattering from a soliton-induced RI*. Finally, we consider the case in which the soliton is accompanied by a second, delayed probe pulse. This second pulse is much weaker and therefore does not form a soliton or excite any nonlinear Kerr effects. Figure 4 shows the results for a 1.9 μm central wavelength probe pulse, pulse width 8 fs and input intensity 5×10^9 W/cm^2 (complete movie showing the full dynamics is also included). The probe pulse is scattered by the soliton induced RI shown in Fig. 3(a)–(b). The initial probe pulse delay, $t_0 = 15$ fs, is adjusted such that it encounters the soliton when it forms the steepest shock-front and is then scattered relatively efficiently, simultaneously spectrally recoiling to a slightly red-shifted wavelength and emitting two blue-shifted RR and NRR modes. In Fig. 4(c) we show the overall photon number evolution for the probe pulse (black solid line) and for the soliton pulse (blue dashed curve). In order to highlight the cross-scattering dynamics, the two curves have been normalized at each propagation distance with respect to two independent simulations for the probe and soliton pulses alone. We thus note that the overall probe pulse photon number increases by nearly 1%, followed by some weaker oscillations that are originating from a remnant of the probe pulse that is trapped and thus continuously interacts with the soliton [see Fig. 4(a), trapped light is visible for $z > 1.5$ mm, around $t \sim 0$ fs]. This clear photon number increase thus indicates that soliton-induced scattering in this regime, very differently from standard cross-phase modulation, may lead to true amplification of the weaker pulse.

Discussion

Summarising, we have shown that a RI amplifies and scatters light to higher frequencies. Likewise, if the probe pulse were to be reduced to

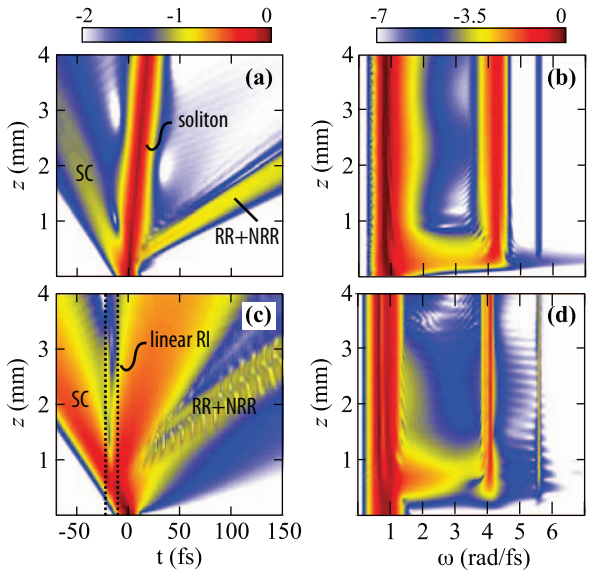

Figure 3 | RI scattering dynamics in fused silica. Comparison between a soliton-induced (via the *nonlinear* Kerr effect) RI (a)–(b) and the "toy-model" RI with the same shape as the soliton-induced inhomogeneity, in a purely linear medium (c)–(d). Envelope (left hand side), and spectral (right hand side) evolution in propagation.

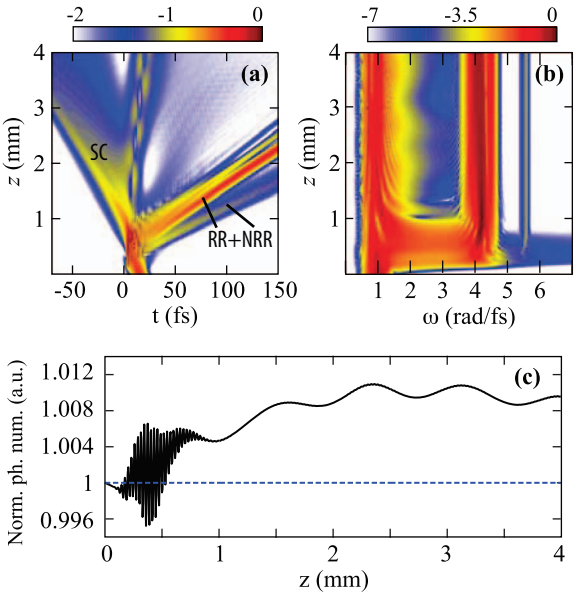

Figure 4 | Weak probe scattering in fused silica, from the soliton-induced RI of Fig. 3(a)–(b). Probe envelope (a) and spectral evolution in propagation (b). Normalised photon number evolution (c) for the probe (black solid curve) and for the soliton (blue dashed curve). A complete movie animation is included.

the level of quantum fluctuations, we may expect to see the RI excite the vacuum states. Bearing in mind that the motion of photons in the vicinity of a RI may also be described in terms of an effective curved space-time metric[21,22], we expect that measurements of vacuum fluctuations excited by a RI would give an experimental direct window into the physics of the quantum vacuum in curved space-times[23–25].

These results therefore open the perspective for novel all-optical control schemes that may be implemented in a wide variety of geometries and applications together with a novel numerical and experimental approach for the investigation of fundamental phenomena.

Methods

Numerical model. The code adopted for the numerical results presented in the main text is a 1D Unidirectional Pulse Propagation Equation (UPPE) solver[19], where the spectral components $E_\omega(z)$ of the real field $E(z, t)$, are obtained by Fourier transform and obey to the following model equation, in the pulse or inhomogeneity comoving frame:

$$\partial_z E_\omega - i[k_z(\omega) - \omega/v]E_\omega = i\frac{\omega^2}{2\epsilon_0 c^2 k_z(\omega)}P_\omega, \tag{4}$$

being ϵ_0 the vacuum permittivity, c the speed of light in vacuum, and P_ω the spectral component at frequency ω of the real-valued polarization as obtained by Fourier transform.

Dispersion of the medium is described by $k_z(\omega)$ and the shift $-\omega/v$ indicates that Eq. (4) is solved in the local frame of the scatterer. Below we report the "linear" (i) and "nonlinear" (ii) implementation of the polarization source term.

(i) - *"Linear source term"*. For the numerical results shown in Fig. 2 and in Fig. 3(c)–(d), the polarization source term is implemented as a linear relativistic inhomogeneity (RI), travelling at velocity v along the z direction, i.e.,

$$P(z, t) = \epsilon_0\left\{[n_0 + \delta n(t - z/v)]^2 - n_0^2\right\}E(z, t), \tag{5}$$

where the background term, n_0, is the refractive index at the input carrier frequency and $\tau = t - z/v$ is the local time coordinate. The "artificial" RI (δn) has a super-Gaussian longitudinal profile of amplitude δn_0 and thickness σ: $\delta n(\tau) = \delta n_0 \exp[-(\tau - t_0)^m/\sigma^m]$; being m a positive even number identifying the Gaussian order and t_0 the initial temporal position.

(ii) - *"Nonlinear source term"*. The numerical model is extended to include the nonlinear case presented in Fig. 3(a)–(b); that is the case in which the inhomogeneity is induced by an intense soliton through the nonlinear Kerr effect. The polarization source term is $P(z, t) = \epsilon_0 n_0 n_2 |\mathcal{E}(z, t)|^2 E(z, t)$ where $\mathcal{E}$ is the complex valued analytical signal and $(1/2)n_2|\mathcal{E}(z, t)|^2$ gives the dimensionless refractive index variation.

The probe pulse scattering by the soliton-induced RI, is modelled by solving a second equation for the real field of the probe pulse, $E_2(z, t)$, coupled to the equation for the soliton (4):

$$\partial_z E_{2,\omega} - i[k_z(\omega) - \omega/v]E_{2,\omega} = i\frac{\omega^2}{2\epsilon_0 c^2 k_z(\omega)}P_{2,\omega}. \tag{6}$$

The coupling is indeed given by the "cross-phase modulation" term of the nonlinear polarization, i.e., $P_2(z, t) = 2\epsilon_0 n_0 n_2 |\mathcal{E}(z, t)|^2 E_2(z, t)$, where $\mathcal{E}$ is the complex valued analytical signal of the pump (soliton), as in the previous case.

We intentionally neglect all the other nonlinear terms, e.g. third harmonic generation and Raman scattering, in order to highlight the generation of the RR and NRR modes. Moreover, we recall that, in order to capture the coupling between positive and negative frequencies, the model equation (and especially the source term), must be implemented by calculating the ω-frequency component of the *real* polarization $P(z, t)$. This is achieved for each propagation step by means of back and forth Fourier transforms allowing for an evaluation of the real electric field $E(z, t)$ from its complex spectral components $E_\omega(z)$.

1. Mendonça, J. T. *Theory of photon acceleration* (Institute of Physics Publishing, Bristol, 2001).
2. Rosanov, N. N. Radiation reflection from inhomogeneities moving in a medium with a plasma dispersion law. *Opt. Spectrosc.* **106**, 742 (2009).
3. Savage, R. L., Joshi, C. & Mori, W. B. Frequency upconversion of electromagnetic radiation upon transmission into an ionization front. *Phys. Rev. Lett.* **68**, 946–949 (1992).
4. Gaburro, Z., Ghulinyan, M., Riboli, F., Pavesi, L., Recati, A. & Carusotto, I. Photon energy lifter. *Opt. Express* **14**, 7270–7278 (2006).
5. Preble, S. F., Xu, Q. & Lipson, M. Changing the colour of light in a silicon resonator. *Nature Photon.* **1**, 293–296 (2007).
6. Kampfrath, T., Beggs, D. M., White, T. P., Melloni, A., Krauss, T. F. & Kuipers, L. Ultrafast adiabatic manipulation of slow light in a photonic crystal. *Phys. Rev. A* **81**, 043837 (2010).
7. Boyd, R. W. *Nonlinear Optics* (Academic Press, Elsevier, 2008).
8. Philbin, T. G., Kuklewicz, C., Robertson, S., Hill, S., König, F. & Leonhardt, U. Fiber-optical analog of the event horizon. *Science* **319**, 1367 (2008).
9. Demircan, A., Amiranashvili, Sh. & Steinmeyer, G. Controlling Light by Light with an Optical Event Horizon. *Phys. Rev. Lett.* **106**, 163901 (2011).
10. Akhmediev, N. & Karlsson, M. Cherenkov radiation emitted by solitons in optical fibers. *Phys. Rev. A* **51**, 2602 (1995).
11. Wai, P. K. A., Menyuk, C. R., Lee, Y. C. & Chen, H. H. Nonlinear pulse propagation in the neighborhood of the zerodispersion wavelength of monomode optical fibers. *Opt. Lett.* **11**, 464–466 (1986).
12. Tartara, L., Cristiani, I. & Degiorgio, V. Blue light and infrared continuum generation by soliton fission in a microstructured fiber. *Appl. Phys. B* **77**, 307–311 (2003).
13. Skryabin, D. V. & Yulin, A. V. Theory of generation of new frequencies by mixing of solitons and dispersive waves in optical fibers. *Phys. Rev. E* **72**, 016619 (2005).
14. Dudley, J. M., Genty, G. & Coen, S. Supercontinuum generation in photonic crystal fiber. *Rev. Mod. Phys.* **78**, 1135 (2006).
15. Rubino, E., McLenaghan, J., Kehr, S. C., Belgiorno, F., Townsend, D., Rohr, S., Kuklewicz, C. E., Leonhardt, U., König, F. & Faccio, D. Negative frequency resonant radiation. *Phys. Rev. Lett.* **108**, 253901 (2012).
16. Kolesik, M., Tartara, L. & Moloney, J. V. Effective three-wave-mixing picture and first Born approximation for femtosecond supercontinua from microstructured fibers. *Phys. Rev. A* **82**, 045802 (2010).
17. Ostrovskii, L. A. Some general relations for waves at the moving boundary between two media. *Soviet Phys. JETP* **34**, 293 (1972).
18. Kravtsov, Y. A., Ostrovskii, L. A. & Stepanov, N. S. *Proc. IEEE* **62**, 1492 (1974).
19. Kolesik, M. & Moloney, J. V. Nonlinear optical pulse propagation simulation: From Maxwell's to unidirectional equations. *Phys. Rev. E* **70**, 036604 (2004).
20. Agrawal, G. P. *Nonlinear Fibre Optics* (Academic Press, New York, 1989).
21. Faccio, D. Laser pulse analogues for gravity and analogue Hawking radiation. *Contemp. Phys.* **53**, 97 (2012).
22. Barceló, C., Liberati, S. & Visser, M. Analogue Gravity. *Living Rev. Relativity* **14**, 3 (2011).
23. Birrell, N. D. & Davies, P. C. W. *Quantum fields in curved space* (Cambridge University Press, Cambridge, 1982).
24. Belgiorno, F., Cacciatori, S. L., Clerici, M., Gorini, V., Ortenzi, G., Rizzi, L., Rubino, E., Sala, V. G. & Faccio, D. Hawking Radiation from Ultrashort Laser Pulse Filaments. *Phys. Rev. Lett.* **105**, 203901 (2010).
25. Rubino, E., Belgiorno, F., Cacciatori, S. L., Clerici, M., Gorini, V., Ortenzi, G., Rizzi, L., Sala, V. G., Kolesik, M. & Faccio, D. Experimental evidence of analogue Hawking radiation from ultrashort laser pulse filaments. *New J. Phys.* **13**, 085005 (2011).

Acknowledgments

D.F. and U.L. acknowledge financial support from the Engineering and Physical Sciences Research Council EPSRC, Grants EP/J00443X/1 and EP/J004200/1.

Author contributions

D.F. and E.R. developed the ideas and performed the numerical simulations. A.L. and A.C. implemented the numerical codes, F.B. and S.C. provided the mathematical models. All authors contributed to the manuscript preparation.

Additional information

Supplementary information accompanies this paper at http://www.nature.com/scientificreports

Competing financial interests: The authors declare no competing financial interests.

How to cite this article: Rubino, E. *et al.* Soliton-induced relativistic-scattering and amplification. *Sci. Rep.* **2**, 932; DOI:10.1038/srep00932 (2012).